

Exploring Coronal Heating Using Unsupervised Machine-Learning

Shabbir Bawaji,¹ Ujjaini Alam,¹ Surajit Mondal,² and Divya Oberoi²

¹*Thoughtworks India, Pune, MH, India; shabbirb@thoughtworks.com ,
ujjaini.alam@thoughtworks.com*

²*National Centre for Radio Astrophysics - Tata Institute of Fundamental
Research, Pune, MH, India; surajit@ncra.tifr.res.in , div@ncra.tifr.res.in*

Abstract. The perplexing mystery of what maintains the solar coronal temperature at about a million K, while the visible disc of the Sun is only at 5800 K, has been a long standing problem in solar physics. A recent study by Mondal et al. (2020) has provided the first evidence for the presence of numerous ubiquitous impulsive emissions at low radio frequencies from the quiet sun regions, which could hold the key to solving this mystery. These features occur at rates of about five hundred events per minute, and their strength is only a few percent of the background steady emission. One of the next steps for exploring the feasibility of this resolution to the coronal heating problem is to understand the morphology of these emissions. To meet this objective we have developed a technique based on an unsupervised machine learning approach for characterising the morphology of these impulsive emissions. Here we present the results of application of this technique to over 8000 images spanning 70 minutes of data in which about 34,500 features could robustly be characterised as 2D elliptical Gaussians.

1. Introduction

The solar atmosphere, known as the corona, is at a temperature of about a million K, while the visible disc of the Sun, the photosphere, is only at 5800 K. What maintains the coronal temperature so much hotter than the photosphere still remains a puzzle and has come to be known as the *coronal heating problem*. A promising resolution to the problem is now known as the *nanoflare hypothesis*, which proposes the presence of a large number of tiny flares taking place all over the Sun all the time, too weak to be detected individually but collectively with sufficient energy to heat up the corona (Parker 1988). Generations of ever more sensitive X-ray and extreme-UV telescopes have however so far been unable to detect these nanoflares. A key consequence of this hypothesis is the ubiquitous presence of very weak impulsive emissions in the metre-wave radio band. The very first detection of these emissions has recently been reported by Mondal et al. (2020). We refer to these emissions as Weak Impulsive Narrow-band Quiet Sun Emissions (WINQSEs). As a step towards exploring in greater detail the suitability of WINQSEs for explaining coronal heating, here we attempt to characterise their morphology. They have been detected with sufficient SNR in these high fidelity and high time resolution radio images to allow a robust characterisation. Given the vast volumes of data and the large number of WINQSEs which need to be examined, one necessarily requires a robust automated approach. Here we present a machine learning

based algorithm which meets these requirements and characterises the morphologies of WINQSEs using a 2D elliptical Gaussian model.

2. Data

These data span 70 minutes and come from the Murchison Widefield Array (Tingay et al. 2013) during a period of low solar activity. They were imaged with a time and frequency resolution of 0.5 s and 160 kHz, leading to over 8000 images at 132 MHz. The lone active region present on the visible disc of the Sun appears as the brightest radio source. Some of the images were completely dominated by the emission from this region. Such images and the emission from this region are not used for this study.

3. Methodology

The input for our pipeline is a spatio-temporal solar data cube $I(x, y, t)$, where I denotes the flux density, x and y are the spatial coordinates in the image and t the time. We start by empirically defining a solar boundary within which to search for peaks. We define a mean image, P , over time ($P_{x,y} = \frac{1}{T} \sum_{t=1}^T I_{x,y,t}$) and the region in P with intensity $> 0.002 \times P_{max}$ is defined to be the Sun. The same region is used in all the images as the solar boundary. To avoid working with image features observed with poor Signal to Noise Ratio (SNR), we impose a constraint of $SNR > 5$, where SNR is determined from the RMS fluctuations in the map at a location far from the Sun.

On an average, each image has about 10 weak features. Naturally some of them tend to be clustered and overlap in the images, making it harder to model the morphology of individual WINQSEs. For ease of morphological characterization, we focus here on the isolated peaks. To do this efficiently, we use Density-Based Spatial Clustering of Applications with Noise (DBSCAN), an unsupervised, non-parametric clustering algorithm (Ester et al. 1996). Given a set of points in some parameter space, this algorithm groups together points with many nearby neighbours, and isolated points lying in regions of low-density are treated as outliers. Here, DBSCAN is applied such that if at least two peaks are less than 5 pixels apart they are regarded as a cluster, and the peaks that are farther apart are marked as isolated ones by the algorithm.

The next step is to find an optimal window size for fitting Gaussians to the individual peaks. A window that is too small would not have enough information for a successful fitting, while a large window could potentially include contaminating emission from neighboring peaks. During peak finding, the identified peaks are characterized by multiple parameters – peak amplitude, peak importance (difference between the peak and the average surrounding flux), distance to the next nearest peak, peak SNR, etc. We transform this many-parameter system to a two-parameter system using t-distributed Stochastic Neighbor Embedding or tSNE (van der Maaten & Hinton 2008). This algorithm is a nonlinear dimensionality reduction technique that models each higher dimensional object by a two-dimensional point. It calculates the probabilities of similarity between points in the higher and lower dimensional spaces, then minimizes the difference between these probabilities. This leads to an accurate two-dimensional representation of the original data. The lower dimensional data is now clustered using DBSCAN and the optimal fitting window-size of each cluster is determined to be the median nearest-neighbour-distance for that cluster.

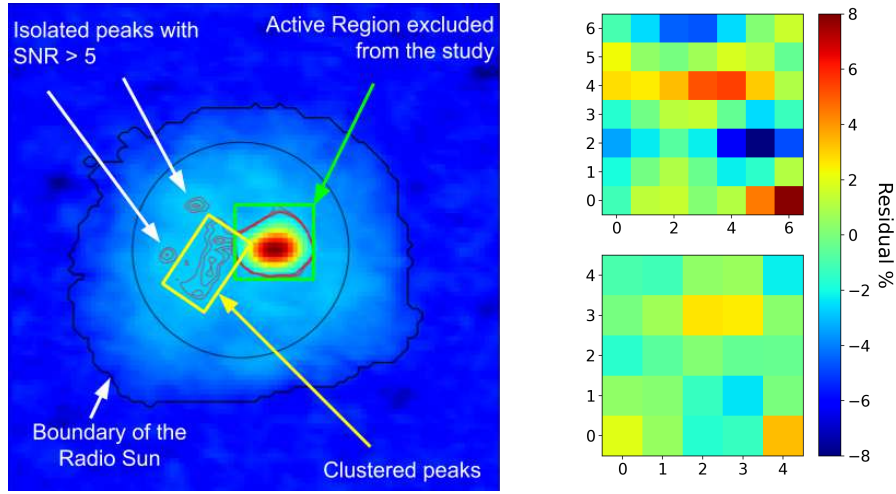


Figure 1. The left panel shows a typical radio image of the Sun. Solar boundary in visible and radio parts of the spectrum are marked. Examples of both isolated and clustered peaks are indicated. The right panel shows the residuals for the two isolated peaks fit by the 2D elliptical Gaussian model.

We find that a 2D elliptical Gaussian, defined below, provides a good description for the vast majority of isolated features.

$$I = O + A \frac{2}{\pi^2 \sigma_x \sigma_y} e^{\left[-\frac{1}{2} \left(\frac{1}{\sigma_x} [(x-x_0) \cos \theta - (y-y_0) \sin \theta] \right)^2 - \frac{1}{2} \left(\frac{1}{\sigma_y} [(y-y_0) \cos \theta + (x-x_0) \sin \theta] \right)^2 \right]}$$

where O is the offset, A the amplitude, σ_x, σ_y the widths of the major and minor axes, x_0, y_0 the position of the Gaussian peak, and θ its angle of orientation with respect to the x-axis.

The algorithm further rejects outliers with large errors on the Gaussian fit parameters, or with a large χ^2 , and outputs a set of Gaussian parameters that can be used to characterize WINSQEs. An example radio image is shown in Fig. 1 along with the residuals for the best fit Gaussian fits to the two isolated features. The residuals are only at a few percent, confirming that the peaks are described well by the Gaussian models.

4. Results

A total of 70,845 peaks were found with $SNR > 5$. Of these, 42,469 were identified to be isolated. The χ^2 for Gaussian fits to 34,457 of these peaks were found to be acceptably low. Figure 2 shows the distributions of intensity, area, axial ratio and major axis of the best fit Gaussian parameters. The size and areas of the Gaussian models show that their emissions are quite compact, with median area of ~ 24 and median major axis width of ~ 4 in pixel units, while the angular resolution of these observations is ~ 14 in the same units. This is in line with theoretical expectations. Each of these distributions show a small number of outliers with unphysically large values, these are under investigation.

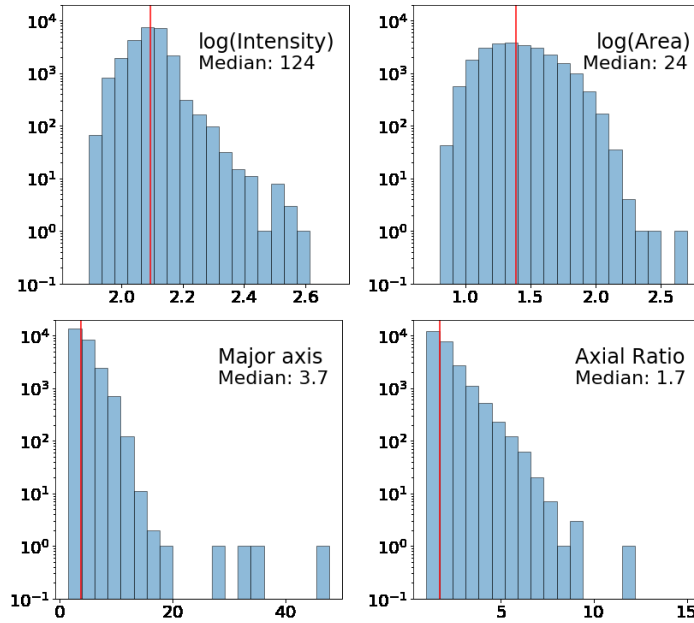


Figure 2. Distributions of the best fit Gaussian parameters for the WINSQEs (intensity, area, major axis and axial ratio). The median values are mentioned in linear units and marked by a vertical red line in each of the panels.

5. Conclusions

The algorithm presented here successfully distinguishes between the weak isolated and clustered emissions and provides a robust characterisation of the shapes of isolated WINQSEs. The modeled characteristics are found to be in line with the theoretical expectations for the origin of WINQSEs. Our immediate next step will be to test the robustness of the pipeline with additional data-sets. From a science perspective, it will be very interesting to study the evolution of morphology of these sources across both time and frequency axes, and the MWA is capable of providing data suitable for such an exploration. We plan to expand the scope of this work to meet this objective.

Acknowledgments. SB acknowledges H. Hayatnagarkar, S. Khandekar, D. Singh and S. Surana, all from Thoughtworks India, for useful discussions.

References

- Ester, M., Kriegel, H.-P., Sander, J., Xu, X., et al. 1996, in *Kdd*, vol. 96, 226
Mondal, S., Oberoi, D., & Mohan, A. 2020, *ApJ*, 895, L39. 2004.04399
Parker, E. N. 1988, *ApJ*, 330, 474
Tingay, S. J., Goeke, R., Bowman, J. D., Emrich, D., et al. 2013, *PASA*, 30, e007. 1206.6945
van der Maaten, L., & Hinton, G. 2008, *Journal of Machine Learning Research*, 9, 2579. URL <http://www.jmlr.org/papers/v9/vandermaaten08a.html>